J. King Saud Univ., Vol. 15, *Comp. & Info. Sci*., pp. 1-31 (A.H. 1423/2003)

Surface Reconstruction from Multiple Views of Painted Curves

Madasu Hanmandlu, V. Shantaram* and M. Vamsi Krishna**
FOE, Multimedia University, Jalan Multimedia, 63100 Cyberjaya Selangor, Malaysia
** IT Department, American InterCon. University, 12655 W. Jefferson Blvd., Los Angeles, USA*
*** Electronics & Communications Dept., S.S.N. College, Ongole 523001, A. P., India*

(Received 12 August 2000; accepted for publication 2 January 2002)

Abstract. A normal to the extremal contour of a 3D object is the same as the normal computed for the image contour projected on the unit sphere by the rays grazing the extremal contour. This fact is utilized in the present work to derive the parameters of quadric surfaces. We require three views of the point of intersection of two painted curves on an object. Out of the three views, one view must be chosen such that the image contours of the curves appear close to the extremal contours. Then the normals to the image contours (i.e., apparent contours) and the normals to the surface curves (i.e., contour generators) can be related through differential geometry to yield quadric representation of a surface at the point of interest.

1. Introduction

The problem of analyzing a sequence of monocular images (intensity or range) or stereo images to extract three dimensional motion and structure is an active area of research in computer vision. While analyzing monocular images reliable tokens (features) such as curves, corners are detected from the spatial variation of image intensities, assuming that they correspond to markings on 3D objects. Second, these tokens are tracked over time to recover depth and 3D velocities of the corresponding 3D tokens. One possibility is to consider two-dimensional tracking, which gives us matches between different frames, and to use these matches for estimating three-dimensional motions. For some of the work published for recovering motion and structure from n point matches, p line matches, between q views where typically n is 5, p is 6 and q is 2 or 3 refer to [1-8]. Three-dimensional tracking is the other possibility [9, 10]. A review on the computation of motion from a sequence of images is given in [11].

Some of the recent works on structure from motion are briefly reviewed in the following: Weng *et al.* [12] determine the structure and motion by minimizing the nonlinear objective function. The error in the optimal solution is compared with a theoretical lower bound. Taylor and Kriegman [13] also estimate the structure of scene composed of straight-line segments by minimizing a nonlinear objective function. This gives the disparity between the observed line segments and the predicted lines. The minimization is done with respect to both the line parameters and camera positions. Seales and Faugeras [14] have designed a working system for reconstructing the surface model for an object that has smooth and sharp surface boundaries. Using either known or computed motion, an image sequence is generated with edges arising out of occluding boundaries. Then the locally reconstructed surface information over multiple views is fitted with a global surface mesh approximating the original 3D object. Reconstruction of 3D structure undergoing rotational motion with respect to camera is presented in [15] knowing the correspondences of the point features tracked over many images. The location of points under perspective projection is found from the computed image trajectories. Wu *et al.* [16] have presented a robust approach to estimate the kinematics of camera and structure of the objects using noisy monocular image sequences. The motion is represented by rectilinear motion parameters whereas the structure parameters are the 3D coordinators of the salient feature points. Then the incremental motion and structure are estimated by both the iterated extended Kalman filter and the nonlinear least squares method. Making an assumption that two matched line segments contain the projection of a common part of the line segment in space to match line segments between different views, Zhang [17] presents an algorithm for recovering motion and structure from two perspective images.

A lot of work has been reported using stereo images to reconstruct a depth [10, 18-20]. The main problem in these methods is to establish correspondence between the images and to construct a dense depth map. A review of all types of feature correspondences in monocular and stereo sequence of images for motion and structure can be found in [21].

Visible surfaces viewed from a single viewpoint when stationary yield almost no information about the depth but yield vivid 3D impressions when subjected to movement. This introduces the paradigm called `structure from motion'. The emphasis of structure from motion is to determine the number of views needed to recover the spatial configuration of the scene points and the number of image points or tokens to establish correspondence.

Reconstruction of a surface gives potentially useful information for navigation, grasping and object identification tasks. The present study is aimed at reconstructing quadratic surfaces. There are a number of basic approaches to find a representative description of a surface. Surface curvature along extremal boundaries and the

deformation of an apparent contour (the silhouette of a smooth surface or the image of the extremal contour) under viewer motion is a rich source of geometric information of the object. Barrow and Tenenbaum [22] have shown that the surface orientation along an extremal contour can be computed directly from image data. Koenderink [23] has related the curvature of an apparent contour to the curvature of a surface, i.e.. Gaussian curvature wherein convexities, concavities and inflection of apparent contour indicate respectively convex, hyperbolic or parabolic surface points. Giblin and Weiss [24] have extended this method by adding viewer motions to obtain qualitative estimates of Gaussian curvature.

The objective of the present work is to develop a mathematical formulation using differential geometry for the reconstruction of a visible smooth surface and to show how an active monocular viewer making deliberate exploratory movements can recover reliable descriptions of visible surface geometry from the images of painted curves in different views. Cooper *et al*. [25] have also solved this problem for the reconstruction of a planar surface and their method requires the camera geometry for finding the affine transformation to match the images of painted curves in two or more views. By making use of extremal contours (or, curves in the vicinity of extremal contour) in different views, we are in a way considering the planar curves for the reconstruction of a curved surface.

In this work rather than estimating curvature from the deformation of apparent contours as in [26], we determine the surface parameters from the normal and its derivatives at a point formed by intersecting painted curves. The viewpoints are chosen so that the image contours appear close to the extremal boundary. This will facilitate in relating the normal to the surface curve with the normal to the image contour of the same. This work establishes new identities between a surface normal and a normal to the image contour. Thus the main aim of this paper is to find and verify a new method to reconstruct quadratic surfaces from static contours using differential geometry.

The organization of this is as follows: In section 1, we discuss the imaging model, properties of extremal contours. Section 2 deals with surface reconstruction from static contours. Section 3 presents the results of simulation as well as implementation on an actual object. Conclusions are relegated to Section 4.

1.1 Imaging model

The orientation of any ray can be determined by a monocular observer when it is projected on its imaging surface. However, the observer cannot determine the distance along the ray of the object feature. By choosing the direction of an incoming ray to represent a unit vector, determination of ray's direction is equivalent to considering the imaging device as a spherical pinhole camera of unit radius.

For the spherical projection, let the direction of ray to a world point P with a position vector r(s, t) be a unit vector on the image sphere Q(s, t), defined at time 't' by

$$r(s, t) = v(t) + \lambda (s, t)\, Q(s, t) \tag{1.1}$$

Where $\lambda(s,t)$ is the distance along the ray to the viewed point P and v(t) is the viewer's position as shown in Fig.1.

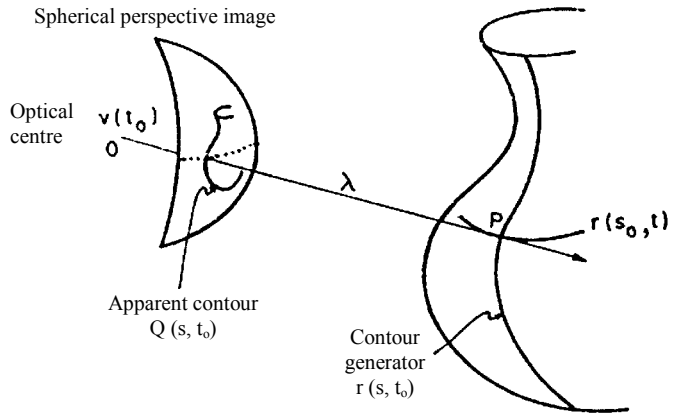

Fig. 1. Spherical projection geometry.

For a given vantage position t_o, the apparent contour $Q(s, t_o)$ is a continuous family of rays emanating from the camera's optical centre which touch the surface forming the contour generator $r(s, t_o)$, as shown in Fig.1, so that

$$Q.n = 0 \tag{1.2}$$

where n is the surface normal.

The tangent to the contour generator is also perpendicular to the normal

$$r_s.\, n = 0 \tag{1.3}$$

As a result, the moving observer at position v (t) sees a two parameter family of apparent contours Q(s,t) as depicted in Fig. 2. Note that Q is the direction of the light ray in the fixed reference frame (world frame)R^3. It is determined by a spherical image position vector Q' (the direction of the light ray in the camera/viewer coordinate system) and the orientation of the camera coordinate system relative to the reference frame. For a moving observer, the viewer coordinate system moves with respect to the

reference frame. We can, therefore, express the relationships between Q and Q' in terms of a rotation operator R(t)

$$Q = R(t)Q' \tag{1.4}$$

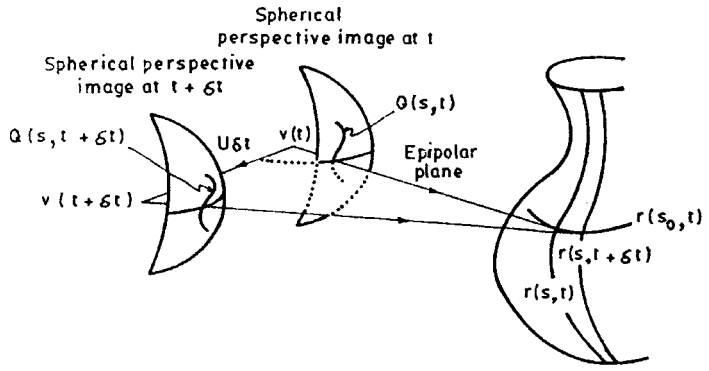

Fig. 2. Epipolar parmeterization.

At $t = 0, Q$ and Q' coincide, at any other t the relative translational and rotational velocities U and Ω are respectively:

$$U = v_t \tag{1.5}$$

$$\Omega \times Q' = R_t Q' \tag{1.6}$$

where the subscript 't' indicates the differentiation with respect to t.

The relation between temporal derivatives of measurements made in the camera coordinate system and those made in the reference coordinate system is obtained by differentiating Q with respect to time denoted as Q_t

$$Q_t = R(t)Q_{t'} + \Omega \times Q'$$

Since at t=0, R(t) is a unity matrix, the above equation becomes

$$Q_t = Q_{t'} + \Omega \times Q' \tag{1.7}$$

1.2 Properties of extremal contour and its projections

We now state the following well-known properties of an extremal contour [27]:

1. The orientation of the surface normal n can be computed by measuring the direction of the ray Q of a point on an extremal contour and the tangent to the apparent image contour Q_s

$$n = \frac{Q \times Q_S}{|Q \times Q_S|} \tag{1.8}$$

2. The ray direction Q and tangent to the extremal contour r_s are in conjugate directions.
   According to the second fundamental form, the ray direction and the extremal contour will only be perpendicular if the ray is along a principal direction.
3. The curvature of the apparent contour K^p can be written in terms of its normal and the derivatives of the image curve as

$$K^p = (Q_{SS}.n) / |Q_S|^2 \tag{1.9}$$

1.3 Representation of apparent contours

As the viewer moves, a family of apparent contours $Q'(s,t)$ is swept out on the image sphere. However, the spatio-temporal parameterization of the family is not unique. The mapping between contour generators and hence between apparent contours at successive instants is underdetermined. To circumvent this problem, use is made of epipolar parameterization defined by

$$r_t \times Q = 0 \tag{1.10}$$

The tangent to the t-parameter curve is chosen to be in the direction of ray, Q. This implies that the grazing/contact point is chosen to `slip' along the ray. Thus the tangent plane basis vectors r_s and r_t are in conjugate directions.

In order to set up correspondence between points on successive snapshots of apparent contour, we differentiate (1.1) with respect to `t' and enforce the epipolar constraint (1.10) leading to

$$Q_t = \frac{(U \times Q) \times Q}{\lambda} \tag{1.11}$$

This indicates that the corresponding ray in the next viewpoint $Q(s_0, t+\delta t)$ is selected so that it lies in the plane defined by (U x Q) - the epipolar plane as shown in Fig.2.

Rewriting eqn (1.11) to yield, λ, we have

$$\lambda = - \frac{U.n}{Q_t.n} \tag{1.12}$$

Thus depth λ (distance along the ray Q) can be computed from the deformation Q_t of the apparent contour under known viewer motion (i.e. translational velocity U).

In terms of measurements on image sphere, (1.11) becomes:

$$Q_t = \frac{(U \times Q') \times Q'}{\lambda} - \Omega \times Q' \tag{1.13}$$

Where Q_t' is the image velocity of a point on the space curve at a distance λ. Equation (1.13) is the well known equation for structure from motion. Points on successive image curves are `matched' by searching along epipolar great circles on the image sphere defined by the viewer motion U, Ω and the image position Q'.

It can be noted from (1.13) that image velocity consists of two components: One is determined by the viewer's rotational velocity about camera centre and is independent of structure of the scene (λ). The second component is determined by the translational velocity of the viewer.

2. Surface Reconstruction from Static Contours

Here the properties of extremal contour are used to derive a relation between the derivative of normal to the contour generator and that of normal to the apparent contour at the point of intersection of painted curves. This relation will provide us some quantities by which the coefficients of the quadratic equation describing the surface can be obtained.

2.1 Relation between the surface normals and curve normals

A surface can be conveniently described by the point (x,y,z) satisfying the following equation:

$$F(x,y,z) = C \tag{2.1}$$

For an explicit function where one of the three coordinates can be expressed in terms of the other two, we can write for z, which is along the optical axis of the camera at the first viewpoint as

$$z = g(x, y) \tag{2.2}$$

For the sake of relating the computed normals and their derivatives at the two viewpoints with respect to a single reference point, we consider the first viewpoint as our reference coordinate system.

In view of (2.2) F can be rewritten as

$$F = (g(x, y) - z + C) \tag{2.3}$$

Therefore,

$$\Delta F = \frac{\partial g}{\partial x} i + \frac{\partial g}{\partial y} j - k$$

$$= \frac{\partial z}{\partial x} i + \frac{\partial z}{\partial y} j - k \qquad (2.4)$$

Denoting $\frac{\partial z}{\partial x}$ by p and $\frac{\partial z}{\partial y}$ by q, we have

$$\Delta F = p\,i + q\,j - k$$

Hence the unit normal at any point is then

$$N = \frac{\Delta F}{|\Delta F|} = \frac{p\,i + q\,j - k}{\sqrt{(p^2 + q^2 + 1)}}$$

$$= N_i\,i + N_j\,j + N_k\,k \qquad (2.5)$$

This gives the relations

$$p = \frac{-N_i}{N_k} \quad \text{and} \quad q = \frac{-N_j}{N_k} \qquad (2.6)$$

Note that n was also referred to as the surface normal in the context of extremal contours in the previous section. In this section, we distinguish between N and n as the former indicating normal to the contour generator and the latter, to the apparent contour.

In the first viewpoint, assume a plane parallel to XY plane cutting the object surface along the vertical painted curve to generate an extremal contour E_1 that is viewed as apparent contour in Fig.3. Here, the extremal contour is our contour generator. Let the normal to this contour generator be N_1, an element on the contour generator be denoted by $ds|_r$ and that on apparent contour be denoted by $ds|_Q$ such that

$$ds|_r = |r_s| = \sqrt{(dx^2 + dy^2)}$$

$$= dx \sqrt{\left[1 + \left(\frac{dy}{dx} \right)^2 \right]} \tag{2.7}$$

$$ds|_Q = |\, Q_S \,| \tag{2.8}$$

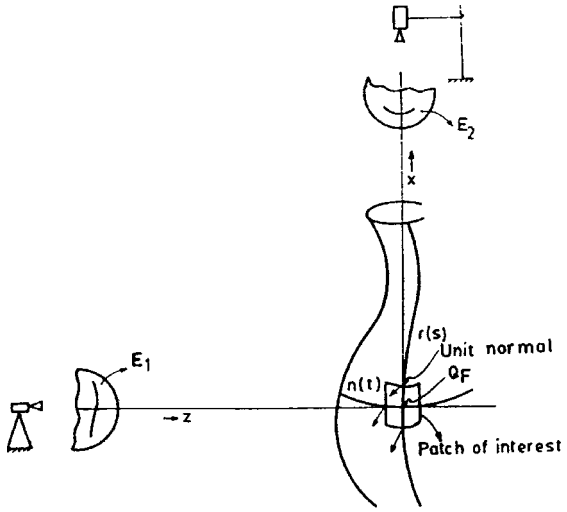

Fig. 3. Two orthogonal views.

Along the contour generator the unit normal N_1 changes its direction. For an infinitesimal change along r with respect to s , $ds|_r$, let the corresponding change in N_1 be dN_1 . Then the partial derivative N_s is given by

$$N_S = \frac{\partial N1}{\partial s|_r} = \frac{\partial N1}{\partial x\sqrt{\left[1 + \left(\frac{dy}{dx}\right)^2\right]}}$$

$$= \frac{\partial N1}{\partial y\sqrt{\left[1 + \left(\frac{dx}{dy}\right)^2\right]}} \tag{2.9}$$

Taking $|\Delta F|$ constant over $ds|_r$ in (2.5), we have

$$\frac{\partial N1}{\partial x} = \frac{1}{|\Delta F|}\frac{\partial \Delta F}{\partial x} = \frac{(\frac{\partial p}{\partial x} i + \frac{\partial q}{\partial x} j)}{\sqrt{(p^2 + q^2 + 1)}} \tag{2.10}$$

From (2.9), $$\frac{\partial N1}{\partial x} = \sqrt{\left[1 + \left(\frac{dy}{dx}\right)^2\right]}\, N_S \tag{2.11}$$

Combining (2.10) and (2.11), we obtain

$$\frac{\partial p}{\partial x} i + \frac{\partial q}{\partial x} j = - N_k' \sqrt{\left[1 + \left(\frac{dy}{dx}\right)^2\right]}\, N_S \tag{2.12}$$

where $N_k' = \frac{1}{N_k}$

Corresponding to $\frac{\partial N1}{\partial y}$, we get from (2.12) as

$$\frac{\partial p}{\partial y} i + \frac{\partial q}{\partial y} j = - N_k' \sqrt{\left[1 + \left(\frac{dx}{dy}\right)^2\right]}\, N_S \tag{2.13}$$

where N_k', N_s and $\frac{dy}{dx}$ can be easily obtained from the apparent contour E_1 as explained below :

Differentiating (1.1) with respect to s, we have

$$r_s = \lambda_s Q + \lambda Q_s \tag{2.14}$$

where we have ignored the arguments. Taking the dot products with the terms in the above equation gives us the following:

$$\lambda_S = r_S \cdot Q$$

$$Q_S = \frac{(r_S - \lambda_S . Q)}{\lambda}$$

$$Q_S . Q_S = \frac{\{| r_S |^2 - (r_S . Q)^2\}}{\lambda^2}$$

$$| Q_S | = \frac{| r_S |}{\lambda} \left[1 - \left\{ \left(\frac{r_S}{| r_S |} \right) . Q \right\}^2 \right]^{1/2}$$

$$| Q_S | = | r_S | \frac{(1 - \cos^2 \theta)^{1/2}}{\lambda} \tag{2.15}$$

$$\text{So, } | Q_S | = \frac{| r_S |}{\lambda} \sin\theta \tag{2.16}$$

where θ is the angle between the ray and the contour generator. Note that the mapping from contour generator to apparent contour is singular when $\theta = 0$. The tangent to the contour generator projects to a point in the image.

Thus, we have from (2.16)

$$ds|_r = \frac{\lambda \; ds|_Q}{\sin\theta} \tag{2.17}$$

In view of (2.17) N_s can be rewritten as

$$N_S = \frac{\partial N1}{\partial s|_r} = \sin\theta \frac{\partial N1}{\lambda \; \partial s|_Q}$$

Since at the extremal contour, the normal to the contour generator N_1 is the same as the normal to the apparent contour n_1 in the first view, so we can write

$$N_S = \left(\frac{\sin\theta}{\lambda}\right)\left(\frac{\partial n1}{\partial s|_Q}\right) = \left(\frac{\sin\theta}{\lambda}\right) n_S \tag{2.18}$$

This result gives a relationship between the derivative of surface normal and that of the image normal. In case of unknown θ, it has to be estimated from n_s in different views. We also have :

$$\frac{dy}{dx} = \frac{Q_S \cdot j}{Q_S \cdot i} = \frac{Q_{sj}}{Q_{si}}$$

The unit image normal n can be computed by measuring the direction of the ray Q of a point on an extremal contour and the tangent to the apparent image contour Q_s

$$n1 = \frac{Q \times Q_S}{|Q \times Q_S|} \tag{2.19}$$

The sign of the normal can only be determined if we know on which side of the apparent contour the surface lies. However, the "sidedness" of the contour can be determined from the deformation of the apparent contour under viewer motion. In the following we choose the convention that the surface normal is defined away from the solid surface. Our intention now is to find the variation of n_1 along apparent contour and relate this to variation in N_1 of the contour generator. Accordingly, n_s is given by

$$n_S = \frac{\partial n1}{\partial s|_Q} = \frac{\partial}{\partial s|_Q}\left[\frac{Q \times Q_S}{|Q \times Q_S|}\right]$$

$$= \frac{Q_S \times Q_S + Q \times Q_{SS}}{|Q \times Q_S|} - \frac{(Q \times Q_S).(Q \times Q_S).(Q_S \times Q_S + Q \times Q_S)}{|Q \times Q_S|^3}$$

$$= \frac{(Q \times Q_{SS})}{|Q \times Q_S|} - \frac{[n1.(Q \times Q_{SS})]n1}{|Q \times Q_S|}$$

$$= \frac{(Q \times Q_{SS}) - [n1 \cdot (Q \times Q_{SS})]\, n1}{|Q \times Q_S|} \tag{2.20}$$

where Q, Q_s and Q_{ss} are the position vectors of an image point, first order derivative and second order derivative of the image curve with respect to parameter s respectively. Q_s is nothing but the tangent to the curve and Q_{ss} is the rate of change of tangent in the image curve.

While deriving (2.12) & (2.13) we have made an assumption that $|\Delta F|$ is constant. If we relax the assumption, we have to proceed to derive the following:

$$\frac{\partial N1}{\partial x} = \frac{\partial}{\partial x}\left[\frac{\Delta F}{|\Delta F|}\right] = \frac{\partial}{\partial x}\left[\frac{p\,i + q\,j - k}{\sqrt{(p^2 + q^2 + 1)}}\right]$$

$$= \frac{\sqrt{(p^2 + q^2 + 1)}\left(\frac{\partial p}{\partial x}\right) - (p\,i + q\,j - k)\,(2p\frac{\partial p}{\partial x} + 2q\frac{\partial q}{\partial x})/\{2\sqrt{(p^2 + q^2 + 1)}\}}{p^2 + q^2 + 1}$$

$$= \frac{\sqrt{(p^2 + q^2 + 1)}\left(\frac{\partial p}{\partial x} i + \frac{\partial q}{\partial x} j\right) - N1\left(p\frac{\partial p}{\partial x} + q\frac{\partial q}{\partial x}\right)}{(p^2 + q^2 + 1)}$$

$$= \frac{\left(\frac{\partial p}{\partial x} i + \frac{\partial q}{\partial x} j\right) - N1\left(Ni\,\frac{\partial p}{\partial x} + Nj\frac{\partial q}{\partial x}\right)}{\sqrt{(p^2 + q^2 + 1)}}$$

$$\frac{\partial N1}{\partial x} = -\,Nk\left[(1 - N_i^2)\,\frac{\partial p}{\partial x} - Ni\,Nj\,\frac{\partial q}{\partial x}\right] i$$

$$- N_k \left[- N_i \; N_j \frac{\partial p}{\partial x} + (1 - N_j^2) \frac{\partial q}{\partial x} \right] j$$

$$- N_k \left[- N_i N_k \frac{\partial p}{\partial x} - N_j \; N_k \frac{\partial q}{\partial x} \right] k \qquad (2.21)$$

Equating $i,\ j,\ k$ components of (2.12) and (2.21)

$$(1 - N_i^2) \frac{\partial p}{\partial x} - N_i \; N_j \frac{\partial q}{\partial x} = - N_k' \sqrt{\left[1 + \left(\frac{dy}{dx} \right)^2 \right]} N_{si}$$

$$(- N_i N_j) \frac{\partial p}{\partial x} + (1 - N_j^2) \frac{\partial q}{\partial x} = - N_k' \sqrt{\left[1 + \left(\frac{dy}{dx} \right)^2 \right]} N_{sj}$$

$$- N_i \; N_k \frac{\partial p}{\partial x} - N_j \; N_k \frac{\partial q}{\partial x} = - N_k' \sqrt{\left[1 + \left(\frac{dy}{dx} \right)^2 \right]} N_{sk} \qquad (2.22)$$

where $\{ \}_i$ denotes the i^{th} component of bracketed term. From (2.22) we can compute $\frac{\partial p}{\partial x}$ and $\frac{\partial q}{\partial x}$. Here we have an overdetermined set of equations with two unknowns and three equations. The third equation is used to refine the estimates of the unknowns.

Similarly, we can derive the following equations from (2.9) using $\frac{\partial N_l}{\partial y}$

$$(1 - N_j^2) \frac{\partial p}{\partial y} - N_i N_j \frac{\partial q}{\partial y} = - N_k' \sqrt{\left[1 + \left(\frac{dx}{dy} \right)^2 \right]} N_{si}$$

$$- N_j\ N_i \frac{\partial p}{\partial y} + (1 - N_i^2)\frac{\partial q}{\partial y} = - N_k' \sqrt{\left[1 + \left(\frac{dx}{dy}\right)^2\right]} N_{sj}$$

$$- N_j\ N_k \frac{\partial p}{\partial y} - N_i\ N_k \frac{\partial q}{\partial y} = - N_k' \sqrt{\left[1 + \left(\frac{dx}{dy}\right)^2\right]} N_{sk} \qquad (2.23)$$

From (2.23) we can compute $\frac{\partial p}{\partial y}$ and $\frac{\partial q}{\partial y}$.

If $\frac{dy}{dx}$ is infinity or a very large number then $\frac{\partial p}{\partial x}$ and $\frac{\partial q}{\partial x}$ can not be computed. If $\frac{dx}{dy}$ is zero or very small number then $\frac{\partial p}{\partial y}$ and $\frac{\partial q}{\partial y}$ can be computed accurately. Similarly if $\frac{dx}{dy}$ is infinity we can not compute $\frac{\partial p}{\partial y}$ and $\frac{\partial q}{\partial y}$ but can compute $\frac{\partial p}{\partial x}$ and $\frac{\partial q}{\partial x}$. If N_k is nonzero, then p and q are finite. Our method requires that N_k should be nonzero and it is nonzero if the k^{th} component of $(Q \times Q_s)$ is nonzero. The k^{th} component is $[Q_i Q_{sj} - Q_j Q_{si}]$. It follows that N_k is nonzero if Q_i or Q_j is nonzero.

As shown in Table 1 by checks, in the worst case of $\frac{dy}{dx}$ being equal to infinity we can get $p, q, \frac{\partial p}{\partial y}$ and $\frac{\partial q}{\partial y}$. On the contrary, if $\frac{dx}{dy}$ is equal to infinity then we can get $p, q, \frac{\partial p}{\partial x}$ and $\frac{\partial q}{\partial x}$. In the best case we can get $p, q, \frac{\partial p}{\partial x}$, $\frac{\partial q}{\partial x}$, $\frac{\partial p}{\partial y}$ and $\frac{\partial q}{\partial y}$. The cross 'x' indicates that we cannot get the corresponding term.

The set of equations (2.22) can be represented as:

$$\begin{bmatrix} 1 - N_i^2 & - N_i N_j \\ - N_i N_j & 1 - N_j^2 \\ - N_i N_k & - N_j N_k \end{bmatrix} \begin{bmatrix} \frac{\partial p}{\partial x} \\ \frac{\partial q}{\partial x} \end{bmatrix} = \begin{bmatrix} - \alpha \ N_{si} \\ - \alpha \ N_{sj} \\ - \alpha \ N_{sk} \end{bmatrix} \tag{2.24}$$

where $\alpha = + N_{k'} \sqrt{\left[1 + \left(\frac{dy}{dx} \right)^2 \right]}$

Table 1. The finite derivatives in the given conditions

	$\frac{dy}{dx} = \infty$	$\frac{dx}{dy} = \infty$	$\frac{dy}{dx} \neq \infty$, $\frac{dx}{dy} \neq \infty$	$N_k = 0$
p	✓	✓	✓	x
q	✓	✓	✓	x
$\frac{\partial p}{\partial x}$	x	✓	✓	x
$\frac{\partial q}{\partial y}$	✓	x	✓	x
$\frac{\partial p}{\partial y}$	✓	x	✓	x
$\frac{\partial q}{\partial x}$	x	✓	✓	x

This is of the form AX = B which can be written as

$$A^T A X = A^T B$$

$$\begin{bmatrix} 1 - N_i^2 & - N_i N_j \\ - N_i N_j & 1 - N_j^2 \end{bmatrix} \begin{bmatrix} \frac{\partial p}{\partial x} \\ \frac{\partial q}{\partial x} \end{bmatrix} = - \alpha \begin{bmatrix} (1 - N_i^2)\ N_{si} - N_i N_j N_{sj} - N_i N_k N_{sk} \\ - N_i N_j N_{si} + (1 - N_j^2) N_{sj} - N_j N_k N_{sk} \end{bmatrix} \quad (2.25)$$

Similarly, we have

$$\begin{bmatrix} 1 - N_j^2 & - N_j N_i \\ - N_j N_i & 1 - N_i^2 \end{bmatrix} \begin{bmatrix} \frac{\partial p}{\partial y} \\ \frac{\partial q}{\partial y} \end{bmatrix} = - \beta \begin{bmatrix} (1 - N_j^2)\ N_{si} - N_j N_i N_{sj} - N_j N_k N_{sk} \\ - N_j N_i N_{si} + (1 - N_i^2) N_{sj} - N_i N_k N_{sk} \end{bmatrix} \quad (2.26)$$

where $\beta = + N_k' \sqrt{\left[1 + \left(\frac{dx}{dy} \right)^2 \right]}$

Substituting for the left hand side of (2.25) from (2.22) leads to :

$$- \alpha \begin{bmatrix} N_{si} \\ N_{sj} \end{bmatrix} = - \alpha \begin{bmatrix} (1 - N_i^2) N_{si} - N_i N_j\ N_{sj} - N_i N_k N_{sk} \\ - N_i N_j N_{si} + (1 - N_j^2) N_{sj} - N_j\ N_k\ N_{sk} \end{bmatrix}$$

Consider the first equation,

$$N_{si} = (1 - N_i^2)\ N_{si} - N_i N_j N_{sj} - N_i\ N_k\ N_{sk}$$

which on simplification leads to

$$= > N_i\ N_{si} + N_j N_{sj} + N_k\ N_{sk} = 0$$

$$=> N . N_S = 0$$

as expected.

2.2 Computation of coefficients of quadratic equation

We assume that a surface is fitted with a quadratic equation. The general form of a quadratic is follows:

$$ax^2 + by^2 + cz^2 + dxy + eyz + fxz + gx + hy + iz + j = 0 \tag{2.27}$$

In order to compute the coefficients a to j of this equation, we obtain the first order partial derivatives with respect to x and y.

The partial derivative of (2.27) with respect to x is

$$2ax + 2czp + dy + eyp + f(z + xp) + g + ip = 0 \tag{2.28}$$

The derivatives of (2.28) with respect to x and y are

$$2a + 2c\left(z\frac{\partial p}{\partial x} + p^2\right) + d\frac{dy}{dx} + e\left(y\frac{\partial p}{\partial x} + p\frac{dy}{dx}\right) + f\left(2p + x\frac{\partial p}{\partial x}\right) + i\frac{\partial p}{\partial x} = 0 \tag{2.29}$$

$$2a\frac{dx}{dy} + 2c\left(z\frac{\partial p}{\partial y} + pq\right) + d + e\left(y\frac{\partial p}{\partial y} + p\right) + f\left(q + x\frac{\partial p}{\partial y} + p\frac{dx}{dy}\right) + i\frac{\partial p}{\partial y} = 0 \tag{2.30}$$

The partial derivative of (2.27) with respect to y is

$$2by + 2czq + dx + e(z + yq) + fxq + h + iq = 0 \tag{2.31}$$

The partial derivatives of (2.31) with respect to x and y are

$$2b\frac{dy}{dx} + 2c\left[pq + z\frac{\partial q}{\partial x}\right] + d + e\left[p + q\frac{dy}{dx} + y\frac{\partial q}{\partial x}\right] + f\left[q + x\frac{\partial q}{\partial x}\right] + i\frac{\partial q}{\partial x} = 0 \tag{2.32}$$

$$2b + 2c\left(z\frac{\partial q}{\partial y} + q^2\right) + d\frac{dx}{dy} + e\left(2q + y\frac{\partial q}{\partial y}\right) + f\left(x\frac{\partial q}{\partial y} + q\frac{dx}{dy}\right) + i\frac{\partial q}{\partial y} = 0 \tag{2.33}$$

So if we have $p, q, \frac{\partial p}{\partial x}, \frac{\partial q}{\partial y}, \frac{\partial p}{\partial y}$ and $\frac{\partial q}{\partial x}$ we can form six equations (2.28) - (2.33)

If a derivative quantity in an equation becomes infinity (∞) then that equation cannot be considered. Table 2 shows by checks the possible number of equations that can be considered under given conditions.

Our method as stated earlier needs a nonzero N_k. As per the Table, in the first view at least four equations can be formed. In the best case we get six equations. The additional equations will be used to refine the estimates. Let us consider the worst case where the number of unknown coefficients is nine and the number of equations is four. We get one more equation by substituting x, y and z in (2.27). So the number of equations is now five. We need at least four more equations to solve the unknowns.

Table 2. The equation that can be formed under possible conditions

Eqn. No.	$N_k = 0$	$\frac{dy}{dx} = \infty$	$\frac{dx}{dy} = \infty$	$\frac{dy}{dx} \neq \infty$, $\frac{dx}{dy} \neq \infty$
2.28	x	✓	✓	✓
2.29	x	x	✓	✓
2.30	x	✓	x	✓
2.31	x	✓	✓	✓
2.32	x	✓	x	✓
2.33	x	x	✓	✓
No. of eqns	0	4	4	6

We can form four additional equations by considering the derivatives at a different point in the same view. But the resulting equations are not independent of the earlier equations, hence the need arises for a second view which can be at any displacement and angle from the first view.

It may be noted that the first view on front or top contributes to a maximum of 6 equations or a minimum of 4 equations. When two views are taken on the same side, these together would give one more equation for depth. Based on this count, we can get a maximum of 13 equations or a minimum of 9 equations if we take two views on the front side and one on the top. Accordingly, from 4 views with two on each side we will get a maximum of 14 equations or a minimum of 10 equations, which include two equations for different depths.

The second view is obtained after rotating the camera in the first view such that Z-axis points upwards and translating the origin of the first viewpoint by $(\Delta x, \Delta y, \Delta z)$ as shown in Fig.4. As a result, the second view is orthogonal to the first one.

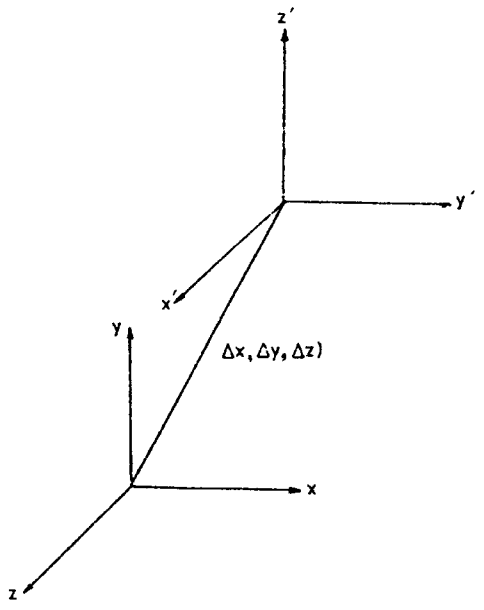

Fig. 4. Relation between the coordinate systems of the two view.

In view of this, (2.27) becomes:

$$\begin{aligned} & a(y'+\Delta x)^2 + b(z'+\Delta y)^2 + c(x'+\Delta z)^2 \\ & + d(y'+\Delta x)\,(z'+\Delta y) + e(z'+\Delta y)\,(x'+\Delta z) \\ & + f(y'+\Delta x)(x'+\Delta z) + g(y'+\Delta x) \\ & + h(z'+\Delta y) + i(x'+\Delta z) + j = 0 \end{aligned} \tag{2.34}$$

where (x', y', z') are the coordinates in the second view.
For the sake of simplicity we will remove the primes. Now, (x, y, z) are the coordinates in the second view. The partial derivatives of (2.34) with respect to x and y are:

$$\begin{aligned} & 2b\,(z+\Delta y)\,p + 2c\,(x+\Delta z) + d\,(y+\Delta x)\,p \\ & + e\,[(z+\Delta y) + (x+\Delta z)\,p] + f\,(y+\Delta x) + hp + i = 0 \end{aligned} \tag{2.35}$$

$$\begin{aligned} & 2a\,(y+\Delta x) + 2b\,(z+\Delta y)\,q + d\left[(y+\Delta x)\,q + (z+\Delta y)\right] \\ & + e\,(x+\Delta z)\,q + f\,(x+\Delta z) + g + hq = 0 \end{aligned} \tag{2.36}$$

The derivatives of (2.35) with respect to x and y are:

$$\begin{aligned} & 2b\left[(z+\Delta y)\,\frac{\partial p}{\partial x} + p^2\right] + 2c + d\left[(y+\Delta x)\frac{\partial p}{\partial x} + p\,\frac{dy}{dx}\right] \\ & + e\left[2p + (x+\Delta z)\,\frac{\partial p}{\partial x}\right] + f\frac{dy}{dx} + h\frac{\partial p}{\partial x} = 0 \end{aligned} \tag{2.37}$$

$$\begin{aligned} & 2b\left[(z+\Delta y)\,\frac{\partial p}{\partial y} + pq\right] + 2c\,\frac{dx}{dy} + d\left[(y+\Delta x)\,\frac{\partial p}{\partial y} + p\right] \\ & + e\left[q + (x+\Delta z)\,\frac{\partial p}{\partial y} + p\frac{dx}{dy}\right] + f + h\,\frac{\partial p}{\partial y} = 0 \end{aligned} \tag{2.38}$$

Differentiating (2.36) with respect to x and y, we get

$$2a\frac{dy}{dx} + 2b\left[(z+\Delta y)\,\frac{\partial q}{\partial x} + pq\right] + d\left[(y+\Delta x)\,\frac{\partial q}{\partial x}\right.$$

$$+ q\frac{dy}{dx} + p \Big] + e\left[(x + \Delta z)\frac{\partial q}{\partial x} + q\right] + f + h\frac{\partial q}{\partial x} = 0 \tag{2.39}$$

$$2a + 2b\left[(z + \Delta y)\frac{\partial q}{\partial y} + q^2\right] + d\left[(y + \Delta x)\frac{\partial q}{\partial y} + 2q\right]$$

$$+ e\left((x + \Delta z)\frac{\partial q}{\partial y} + q\frac{dx}{dy}\right) + f\frac{dx}{dy} + h\frac{\partial q}{\partial y} = 0 \tag{2.40}$$

It may be noted that the derivatives $p, q, \frac{\partial p}{\partial x}, \frac{\partial p}{\partial y}, \frac{\partial q}{\partial x}$ and $\frac{\partial q}{\partial y}$ are different in both the views because of rotation. The derivatives are calculated exactly in the same manner as for the first view.

2.3 Computation of depth at a point

We make use of (1.12) for obtaining the depth at a point. If we make a small translatory motion of the camera along X-axis from the first camera position (first viewpoint), then there will be a corresponding change in the image position. Denoting these changes by Δv_i and $\Delta Q_i'$ then (1.12), assuming any constant, can be written as

$$\lambda 1 = -\frac{\Delta v_i}{\Delta Q_i'} \tag{2.41}$$

The quantities in (2.41) can easily be measured as ΔV_i stands for the movement of camera position along X-axis and $\Delta Q_{i'}$ stands for the change of image point relative to the original point before the translation. It may be mentioned that the above is valid for infinitesimal translatory motion of the camera with unit focal length.
Now, we can write

$$|\lambda| = \frac{\Delta v_i}{\Delta Q_i'}\frac{1}{\rho} \tag{2.42}$$

where ρ is the focal length of the camera. The above formula is an infinitesimal analogue of triangulation with stereo cameras, the numerator is analogous to base line and the denominator to disparity.

2.4 Curvature characteristics

For extremal contours, computations for curvature characteristics can be simplified. These characteristics are derived from the apparent contours in the two

views. The curvature of apparent contour K^p along the s-parameter curve in the first view is given by

$$K^{ps} = \frac{Q_{ss} \cdot n1}{|Q_s|^2} \tag{2.43}$$

where n_1 is normal to the apparent contour. Similarly, the curvature of apparent contour along t-parameter curve in the second view is given by

$$K^{pt} = \frac{Q_{tt} \cdot n2}{|Q_t|^2} \tag{2.44}$$

where n_2 is the normal to the apparent contour in the second view. As the painted curves intersect, the curvatures along the two principal directions are related to the normal curvatures along the corresponding contour generators by the following formula:

$$K^s = \frac{rss \cdot n1}{(rs \cdot rs)} = \left(\frac{\sin^2 \theta 1}{\lambda 1} \right) K^{ps} \tag{2.45}$$

$$K^t = \frac{rtt \cdot n2}{rt \cdot rt} = \left(\frac{\sin^2 \theta 2}{\lambda 2} \right) K^{pt} \tag{2.46}$$

where $\cos\theta 1 = \frac{Q \cdot rs}{|rs|}$ and $\cos\theta 2 = \frac{Q \cdot rt}{|rt|}$. λ_1 and λ_2 are the depths. Note that r_s and r_{ss} are the first and second order derivatives of r along s-parameter curve. Similarly, r_t and r_{rt} are the first and second order derivatives of r along the t-parameter curve.

The Gaussian curvature can be expressed as a product of the normal curvature K^t and the curvature of apparent contour K^{ps} scaled by the depth λ_1. Thus, we have

$$K = \left(\frac{K^{ps}}{\lambda 1} \right) K^t$$

$$= \left(\frac{\sin^2 \theta 2}{\lambda 1 \lambda 2} \right) K^{pt} \; K^{ps} \tag{2.47}$$

The above relation can also be proved alternatively by recognizing that

$$K = \frac{|D|}{|G|} \tag{2.48}$$

where D and G have the following forms :

$$D = \begin{bmatrix} rtt \cdot n1 & rts \cdot n1 \\ rst \cdot n2 & rss \cdot n2 \end{bmatrix}$$

$$G = \begin{bmatrix} rt \cdot rt & rt \cdot rs \\ rs \cdot rt & rs \cdot rs \end{bmatrix}$$

For intersecting painted curves on the object, D and G are turned out to be

$$D = \begin{bmatrix} K^t & 0 \\ 0 & K^s \end{bmatrix}$$

$$G = \begin{bmatrix} 1 & \cos\theta \\ \cos\theta & 1 \end{bmatrix}$$

where $r_{ts}.\ n_1 = r_t\ n_{1s} = 0$. This follows from the tangency condition $Q.n_1 = Q.n_{1s} = 0$
Taking the direction of Q along r_t in $(r_t.\ r_s)$ in the first view, and along r_s in $(r_s.r_t)$ in the second view both of which would yield the same angle θ, we can express K^t and K^s in terms of K^{pt} and K^{ps} as follows:

$$K^t = \left(\frac{\sin^2\theta}{\lambda 2}\right) K^{pt}$$

$$K^s = \left(\frac{\sin^2\theta}{\lambda 1}\right) K^{ps}$$

The mean curvature H and the principal curvatures K_1 and K_2 can be expressed as

$$H = \frac{1}{2}\left[\frac{K^{ps}}{\lambda 1} + \frac{(\sin^2\theta \quad \text{cosec}^2\theta)}{\lambda 2} K^{pt}\right]$$

$$= \frac{1}{2}\left[\frac{K^{ps}}{\lambda 1} + \frac{K^{pt}}{\lambda 2}\right] \tag{2.49}$$

and

$$K_{1,2} = H \pm \sqrt{(H^2 - K)} \tag{2.50}$$

The values of K_1 and K_2 provide the qualitative information about an intersection point on the element surface patch [23].

2.5 Algorithm

Step 1 : Take the image of the object with the vertical painted curve appearing as extremal contour E_1

Step 2 : Extract the extremal contour E_1 of the image using Canny edge operator.

Step 3 : Find the point of intersection of the extremal contour with the horizontal painted curve.

Step 4 : Translate the camera a little and take another image.

Step 5 : Calculate the depth of the object by noting the disparity at the point of intersection.

Step 6 : Fit B-spline curve to the apparent contour E_1

Step 7 : Find the first and second derivatives at the point of intersection along E_1

Step 8 : Calculate unit normal n from (2.19).

Step 9 : Calculate n_s from (2.20)

Step 10 : Calculate N_s from (2.18) taking θ equal to 90^0.

Step 11 : Solve (2.25) for $\frac{\partial p}{\partial x}$ and $\frac{\partial q}{\partial x}$

Step 12 : Solve (2.26) for $\frac{\partial p}{\partial y}$ and $\frac{\partial q}{\partial y}$

Step 13 : Form (2.28) to (2.33) using $p, q, \frac{\partial p}{\partial x}, \frac{\partial q}{\partial x}, \frac{\partial p}{\partial y}, \frac{\partial q}{\partial y}$

Step 14 : Repeat steps 1 to 13 for the second view.

Step 15: Form equations (2.35) to (2.40) using $p,q, \frac{\partial p}{\partial x}, \frac{\partial q}{\partial x}, \frac{\partial p}{\partial y}, \frac{\partial q}{\partial y}$ of the second view.

Step 16 : Solve the equations (2.28) to (2.33), (2.35) to (2.40) and (2.27) using pseudoinverse to get a, b, c, d, e, f, g, h, i.

The computational burden can be reduced for loss of accuracy as follows. Two intersecting curves can be painted on the object and the normal at the point of intersection of both the curves can be considered in both the views. The rate of change of normal at this point can be taken to be equal in both the views. This is true for a spherical surface and they affect widely from each other because the two extremal contour generators may have different slopes.

3. Results of Implementation

The proposed methodology has been implemented on a simulated object, a sphere and a real object, a vase. We have chosen solids of revolution for which the proposed methodology is easily applicable.

3.1 Simulated object

The equation of the sphere is taken to be

$$x^2 + y^2 + z^2 + 10z + 24 = 0$$

The simulated image is stored in a data file in x-y format. The point of interest is arbitrarily chosen.

The parameter `s' of the B spline point at the intersection of image curves Q_F in the front view has been obtained as 82.599. Q_F at s is found to be {0.141, 0.141, -0.98}. The first and second order derivatives at Q_F are calculated using fourth order B-spline function. The derivatives obtained are:

Q_s = { -0.004078, - 0.004082, 0.0 }

Q_{ss} = {0.002358, 0.0, 0.0}

The unit normal n at Q_F is {0.6932, 0.6925, 0.2}.

The slope of the image contour as calculated from $\frac{Q_{sj}}{Q_{si}}$ is -1.001.

The rate of change of image normal at Q_F is, n_s = {3.541, 3.545, 0}

The rate of change of normal at the surface is, $N_s = \frac{n_s}{\lambda}$ = {0.7082, - 0.7090,0}

Using n , N_s and slope, the derivatives $p, q, \frac{\partial p}{\partial x}, \frac{\partial q}{\partial x}, \frac{\partial p}{\partial y}, \frac{\partial q}{\partial y}$

are found to be:

$p = -3.466;\ q = -3.463; \frac{\partial p}{\partial x} = -5.010;\ \frac{\partial q}{\partial x} = 5.018;\ \frac{\partial p}{\partial y} = 5.013;\ \frac{\partial q}{\partial y} = -5.005$

Using these six derivatives, six equations are formed. The same steps as performed in the case of front view are repeated for the image contour in the top view where Q_T is the intersection of the image curves. The following are the results:

For t = 82.599, Q_T at t = {0.141, 0.141, -0.98}

The first derivative is, Q_t = {-0.004078, -0.004082, 0}

The second derivative is, Q_{tt} = {0.0002358, 0.0, 0.0}

The unit normal is n = {0.6932, 0.6925,0.2}

The rate of change of image normal n_t = {3.541,3.545,0}

The rate of change of surface normal N_t = {0.7082, -0.7090,0}

The derivatives are obtained as:

$p = -3.4666$; $q = -3.463$; $\frac{\partial p}{\partial x} = -5.010$; $\frac{\partial p}{\partial x} = 5.018$; $\frac{\partial p}{\partial y} = 5.013$; $\frac{\partial q}{\partial y} = -5.005$

Position vector of the camera in the second view with respect to the first view is (0, 5.0, -5.0). λ is assumed to be 5 in the front view and -5 in the top view.

Six more equations are formed using the above six derivatives. The thirteenth equation is formed by using Q_F. These equations are solved using pseudoinverse to get the nine unknown coefficients. The normalized coefficients of the reconstructed surface are :

a = 1.0 ; b = 0.996 ; c = 0.994 ; d = 0.001 ; e = 0.0 ; f = 0.0 ; g = 0.004 ; h = 0.0 i = 9.942 ; `j = 23.86

The average percentage error in the computed coefficients is 0.87.

This error is small as expected because of the simulated conditions.

The curvature characteristics are also computed as:

$K^{ps} = -4.909$; $K^{pt} = -4.909$; $K^{t} = -1.002$; $K^{s} = -1.002$; $K = 1.004$; $H = -4.909$

$K_{1,2} = -0.1033$, -9.715

As $K_1, K_2 > 0$ the surface point is elliptic as is the case with the spherical object.

3.2 Real object

A camera is mounted on a rotating table whereas the object is placed on the calibrated mount on which it can have a known translation. The object chosen in our experiment has hyperbolic surface at the neck portion, elliptic surface at the bottom portion and parabolic surface at the middle portion of the object. Keeping the camera at a known distance from the intersection of painted curves, the first view is taken such that the vertical painted curve appears as extremal contour. Next, the object is translated and another view is taken for depth calculation. Keeping back the object at the original position the camera is rotated and placed at the same distance from the intersection point such that the horizontal painted curve appears as the extremal contour in the third view. Care must be taken to see that the intersection of painted curves is visible in the first and the third view.

The images are stored in binary format. Fig.5a shows the front view and Fig.5b shows the top view of the object focussing the middle portion of the object . A Canny edge operator, with $\sigma = 9.0$, is applied to these images and their extremal contours are extracted. Figure. 6a shows the extremal contour for the front view and Fig. 6b shows the extremal contour for the top view. The extremal contours are not clear because the surface of the object was glossy and the lights are harsh. In the top view an inner circle is formed because the object is hallow.

After getting the data for extremal contours the coefficients of the quadratic surface have been found to be:

a = 1.0 ; b = 1.001 ; c = 1.061 ; d = -0.163 ; e = 0.138 ; f = -0.0343 ; g = 9.358 ; h = 0.059 ;

i = 155.8 ; j = 5696 ; λ = 79.5 cm

The curvature characteristics are obtained as:

$K^{ps} = 0.0133$; $K^{pt} = 45.42$; $K^{s} = 0.0002506$; $K^{t} = 0.6209$; $K = 0.0001556$; $H = 0.3106$
$K_1 = 0.0003$; $K_2 = 0.6209$

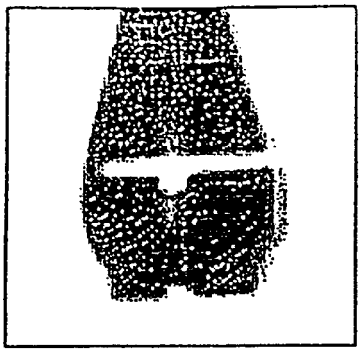

Fig. 5a. Front view of the real object.

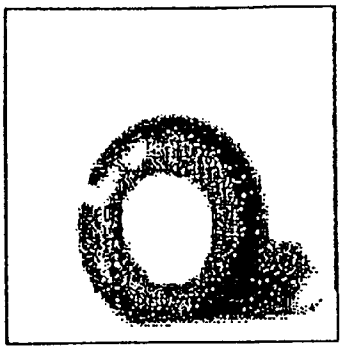

Fig. 5b. Top view of the real object.

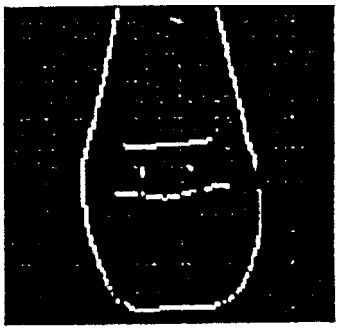

Fig. 6a. Extremal contour of the front view.

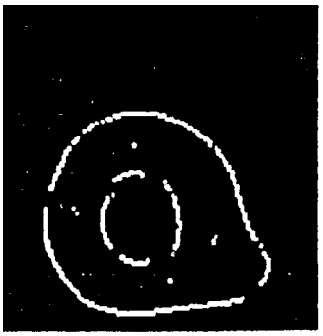

Fig. 6b. Extremal contour of the top view.

Since $K_1 \cong 0$, this indicates that the nature of surface is parabolic as is the case at the point of interest. The coefficients of the quadratic equation provides the structure of the middle portion of the object and the other two portions could not be modeled for non-accessibility of corresponding extremal contours from the second view. However, these can be obtained from the first view as the chosen object belongs to solids of revolution.

4. Conclusion

The proposed method gives a new way of finding surface parameters at a point formed by two intersecting painted curves. While determining these parameters the fact

that the normal to the contour generator is the same as the normal to the apparent contour at the extremal boundary has been made use of.

The first view and the second view need not be orthogonal. They could be at any angle; this would only change (2.34) to (2.40). These equations can be generalized for any angle of rotation. For the special case of solids of revolution, only a single view is enough. This view should be perpendicular to the axis of rotation.

Although the proposed method is powerful in terms of yielding surface reconstruction it cannot provide information on concave surface patches since the curves painted on them cannot be observed as the extremal contours. In such cases, the information from other curves is extremely important though this information is not as powerful as that from the extremal contour case. The present method is also not suitable for highly unsymmetric surfaces for which a large portion of the grid painted on it would be invisible when the rays from camera graze it.

Acknowledgement. The authors wish to express their thanks to Mr.J.S.Kodamala for the computational assistance provided during the implementation of the proposed methodology.

References

[1] Huang, T.S. and Tsai, R.Y. "Image Sequence Analysis: Motion Estimation". In: T.S. Huang, (Eds.). *Image Sequence Processing and Dynamic Scene Analysis*, New York: Springer Verlag, 1981.

[2] Liu, Y. and Huang, T.S. "Estimation of Rigid Body Motion Using Straight Line Correspondences". *Proc. Workshop on Motion: Representation and Analysis*, Charleston, May 1986, 47-51.

[3] Liu, Y. and Huang, T.S. "A Linear Algorithm for Determining Motion and Structure from Line Correspondences". *Comput. Vis. Graph. Image Process*., 44, No.1, (1988), 35-57.

[4] Longuet-Higgins, H.C. "A Computer Algorithm for Reconstructing a Scene from Two Projections". *Nature*, 293 (1981), 33-135.

[5] Tsai, R.Y. and Huang, T.S. " Estimating 3-D Motion Parameters of a Rigid Planar Patch-I". *IEEE Trans. Acoustic. Speech. Sig. Process*, 29, No.6 (1981),1147-1152.

[6] Tsai, R.Y. and Huang, T.S. "Uniqueness and Estimation of Three Dimensional Motion Parameters of Rigid Objects with Curved Surface". *IEEE Trans Patt. Anal. Mach. Intell*., 6, No.1 (1984),13-26.

[7] Ullman, S. *The Interpretation of Visual Motion*. Cambridge MA, MIT Press, 1979.

[8] Yen, B.L. and Huang, T.S. " Determining 3-D Motion/ Structure of a Rigid Body Over 3 Frames Using Straight Line Correspondences". *Proc. Conf. Comput. Vis. Patt. Recog*., Washington, DC, June 19-23, 1983, 267-272.

[9] Bolstein, S.D. and Huang, T.S. "Estimating Motion from Range Data". *Proc. First Conf. AI Applications.* Denver, U.S.A: December, 1984.

[10] Zhang. Z., Faugeras, O.D. and Ayache, N. " Analysis of Sequence of Stereo Scenes Containing Multiple Moving Objects Using Rigidity Constraints". *Proc. 2nd Intern. Conf. Comput. Vis*,. Tampa, FL, December, 1988, 177-186.

[11] Aggarwal, J.K. and Nandha Kumar, N. "On the Computation of Motion from Sequence of Images: A Review". *Proc. IEEE,* 76, No.8 (Aug. 1988), 917-933.

[12] Weng, J., Ahuja, N. and Huang,T.S. " Optimal Motion and Structure Estimation". *IEEE Trans. on Pattern Analysis and Machine Intelligence*, 15, No.9 (Sept.1993), 864-884.

[13] Taylor, C.J. and Kriegman, D.J. "Structure and Motion from Line Segments in Multiple Images". *IEEE Trans. on Pattern Analysis and Machine Intelligence*, 17, No.11 (Nov.1995),1021-1032.
[14] Seales, W.B. and Faugeras, O.D. "Building Three Dimensional Object Models from Image Sequences". *Computer Vision and Image Understanding*, 16, No.3 (May 1995), 308-324.
[15] Sawhney, H.S., Oliensis, J. and Hanson, A.R. "Image Description and 3-D Reconstruction from Image Trajectories of Rotational Motion". *IEEE Trans. on Pattern Analysis and Machine Intelligence*, 15, No. 9 (Sept.1993), 885-898.
[16] Wu,T., Chellappa, R. and Zheng,Q. " Experiments on Estimating Egomotion and Structure Parameter Using Long Monocular Image Sequences". *Int. J. Computer Vision*, 15, No.1/2 (1995), 77-103.
[17] Zhang, Z. "Estimating Motion and Structure from Correspondences of Line Segments Between Two Perspective Images". *IEEE Trans. on Pattern Analysis and Machine Intelligence*, 17, No.12 (Dec. 1995), 1129-1139.
[18] Huang, T.S. and Bolstein, S.D. "Robust Algorithms for Motion Estimation Based on Two Sequential Stereo Image Pairs". *Proc. Conf. Computer Vision and Patt. Recog*, San Francisco, June 19-23, 1985, 518-523.
[19] Zhang, Z. and Faugeras, O.D. " Tracking and Motion Estimation in a Sequence of Stereo Frames". In: Aiello, L.C.(Eds.). *Proc. 9th Europ. Conf. Artif. Intell.*, Stockholm, August 1990, 747-752.
[20] Yachida, M. " 3-D Data Acquisition by Multiple Views". In: Faugeras, O.D. and Giralt, G., (Eds.) *Robotics Research: The Third International Symposium*. Cambridge, MA: MIT press, 1986, pp.11-18.
[21] Huang, T.S. and Netravali, A.N. "Motion and Structure from Feature Correspondences: A Review". *Proc. IEEE,* 82, No.2 (Feb. 1994), 252-268.
[22] Barrow, H.G. and Tenenbaum, J. M. "Recovering Intrinsic Scene Characteristics from Images". In: Hanson, A. and Riseman, E. (Eds.). *Computer Vision Systems*, NY : Academic Press, 1978.
[23] Koenderink, J.J. *Solid Shape.* Cambridge, MA, MIT Press, 1990.
[24] Giblin, P.J. and Weiss, R. "Reconstruction of Surfaces from Profiles". In: *Proc. 1st Intern. Conf. Computer Vision,* London, 1987,136-144.
[25] Cooper, D.B., Huang, Y. and Taubin, G. "A New Model Based Approach for 3-D Surface Reconstruction Using Contours on the Surface Pattern". *Proc. IEEE Conf. on Robotics and Automation*, 1988, 74-83.
[26] Blake, A. and Cippola, R. "Robust Estimation of Surface Curvature from Deformation of Apparent Contours". In: Faugeras, O.D. (Eds). *Proc. Ist European Conf. Computer Vision.* Springer - Verlag., 1990, 465-474.
[27] Cippola, R. *Active Visual Inference of Surface Shape*. Ph.D.Thesis, Univ. of Oxford, 1991.

إعادة بناء مساحة المنحنيات الملونة من خلال مشاهد متعددة

مداسو هانماندلو، ف. شانتا رام* و م. فامسي كرشنا**

ف. أو. أي ، جامعة ملتي ميديا ، جالان ملتي ميديا، ٦٣١٠٠ سايبر جايا، سيلانجر، ماليزيا

** قسم تكنولوجيا المعلومات، الجامعة الأمريكية عبر القارات، ١٢٦٥٥ غرب شارع جيفرسون، لوس انجلوس ، الولايات المتحدة الأمريكية*

*** قسم الاتصالات والإلكترونيات، كلية س. س. ن.، انجولو ٥٢٣٠٠١، اندرابراديش، الهند*

(قدّم للنشر في ٢٠٠٠/٠٨/١٢م؛ وقبل للنشر في ٢٠٠٢/١/٢م)

ملخص البحث. الخط القائم على محيط جسم ثلاثي الأبعاد مماثل للخط القائم المحسوب لمحيط الصورة ذو المسقط على الكرة الأحادية من جرّاء الأشعة الساقطة على المحيط الخارجي. تستعمل هذه الحقيقة في العمل الحالي لاستخراج متغيرات المساحات الرباعية. نحتاج إلى ثلاثة مشاهد لنقطة التقاطع بين منحنيين مرسومين على جسم. يجب أن يكون أحد المشاهد الثلاثة مختار بحيث تكون محيطات صور المنحنيات ظاهرة بقرب المحيطات الخارجية. بعد ذلك، يمكن ربط القوائم على محيطات الصورة بالقوائم على مساحة المنحنيات بواسطة التفاضل الرسمي لإعطاء تمثيل رباعي للمساحة عند النقطة المرغوبة.